Directed evolution of SecB chaperones toward toxin-antitoxin systems

Ambre Julie Sala[a,1], Patricia Bordes[a], Sara Ayala[a], Nawel Slama[a], Samuel Tranier[b], Michèle Coddeville[a], Anne-Marie Cirinesi[a], Marie-Pierre Castanié-Cornet[a], Lionel Mourey[b], and Pierre Genevaux[a,2]

[a]Laboratoire de Microbiologie et de Génétique Moléculaires, Centre de Biologie Intégrative, Université de Toulouse, CNRS, UPS, 31062 Toulouse Cedex 09, France; and [b]Institut de Pharmacologie et de Biologie Structurale, Université de Toulouse, CNRS, UPS, 31077 Toulouse Cedex 04, France

Edited by Linda L. Randall, University of Missouri, Columbia, MO, and approved October 10, 2017 (received for review June 9, 2017)

SecB chaperones assist protein export in bacteria. However, certain SecB family members have diverged to become specialized toward the control of toxin-antitoxin (TA) systems known to promote bacterial adaptation to stress and persistence. In such tripartite TA-chaperone (TAC) systems, the chaperone was shown to assist folding and to prevent degradation of its cognate antitoxin, thus facilitating inhibition of the toxin. Here, we used both the export chaperone SecB of *Escherichia coli* and the tripartite TAC system of *Mycobacterium tuberculosis* as a model to investigate how generic chaperones can specialize toward the control of TA systems. Through directed evolution of SecB, we have identified and characterized mutations that specifically improve the ability of SecB to control our model TA system without affecting its function in protein export. Such a remarkable plasticity of SecB chaperone function suggests that its substrate binding surface can be readily remodeled to accommodate specific clients.

HigB-HigA | SecA | trigger factor | DnaK | Rv1957

In bacteria, the SecB chaperone facilitates protein export via the general Sec pathway by binding to presecretory proteins and maintaining them in a nonnative state competent for translocation through the Sec translocon at the inner membrane (1). SecB bound to its presecretory protein client specifically interacts with the SecA motor subunit of Sec, which subsequently takes over the substrate and promotes its translocation by successive cycles of ATP hydrolysis (2). SecB is mainly present in α-, β- and γ-proteobacteria, but some *secB* sequences are sporadically found in other taxonomic groups, most of which are diderm bacteria (3). Remarkably, over 7% of these *secB* genes are clustered with genes encoding putative type II toxin-antitoxin (TA) systems (1). Type II TA systems are composed of two genes encoding a stable toxin and a less stable antitoxin, where both proteins form a complex in which the toxin is inactive. Under specific stress conditions, the antitoxin is degraded by stress proteases, releasing the active toxin which will act on its intracellular targets and inhibit bacterial growth (4). Such TA-mediated control of growth in response to stress has been involved in several major processes, including biofilm, formation of persister cells, and virulence of several important pathogens (5–8).

The human pathogen *Mycobacterium tuberculosis* possesses such a TA-associated SecB-like chaperone, named *Mtb*-SecB^{TA}, which specifically controls the *Mtb*-HigB1(toxin)-HigA1(antitoxin) TA pair. This system was the first functional tripartite toxin-antitoxin-chaperone (TAC) system identified and is, so far, the most characterized (9, 10). We previously showed that *Mtb*-SecB^{TA} directly interacts with the short carboxyl-terminal extension of *Mtb*-HigA1 antitoxin and protects it from both degradation and aggregation, allowing inactivation of the *Mtb*-HigB1 toxin (9, 11). The toxin *Mtb*-HigB1 of TAC severely inhibits *Escherichia coli*, *Mycobacterium smegmatis*, *Mycobacterium marinum*, and *M. tuberculosis* growth (10), and likely acts as a ribonuclease with a limited number of targets, most of which are involved in iron and zinc homeostasis (12). Despite significant specificity for the antitoxin, *Mtb*-SecB^{TA} likely retains its export chaperone function, as judged by its ability to efficiently replace *E. coli* SecB both in vivo and in vitro (9). However, a direct role for *Mtb*-SecB^{TA} in Sec-dependent protein export in *M. tuberculosis* remains to be demonstrated (a proposed model is illustrated in Fig. S1).

In this study, we have investigated how generic SecB chaperones can specialize toward a TAC antitoxin by recreating such a phenomenon in a directed evolution experiment. Remarkably, we found that single amino acid substitutions within distinct regions of the *E. coli* solitary export chaperone SecB are sufficient to significantly improve its ability to control the *Mtb*-HigBA1 TA pair without affecting its function in protein export.

Results

Directed Evolution of Solitary SecB Toward Control of a TA System. In contrast to *Mtb*-SecB^{TA}, a robust overexpression of the *E. coli* solitary SecB is necessary to suppress the toxicity induced by *Mtb*-HigBA1 (9). We took advantage of this limited suppression by SecB to investigate how a generic export chaperone can specialize toward the control of TA systems. A plasmid library of randomly mutagenized *E. coli secB* was first transformed in the W3110 Δ*secB* strain expressing the *Mtb*-HigBA1 under conditions in which expression of wild-type SecB does not prevent growth inhibition by the toxin, and clones that formed viable colonies were selected for further analysis (Fig. 1*A*). This approach allowed the identification

Significance

Toxin-antitoxin (TA) systems are small genetic modules known to modulate bacterial growth in response to stress. Their major contribution to the formation of persister cells and to the virulence of several important pathogens has highlighted them as promising new targets for therapy. TA-chaperone (TAC) modules are atypical TA systems tightly controlled by a third partner: a molecular chaperone that directly assists the antitoxin. Remarkably, TAC chaperones belong to the family of the canonical SecB chaperone known to facilitate protein secretion in bacteria, thus potentially connecting toxin activation and protein export. Herein, we have used the TAC system of the major human pathogen *Mycobacterium tuberculosis* to reveal how generic chaperones can rapidly evolve to become specialized for TA systems.

Author contributions: A.J.S., P.B., and P.G. designed research; A.J.S., P.B., S.A., N.S., S.T., M.C., and A.-M.C. performed research; M.-P.C.-C. contributed new reagents/analytic tools; A.J.S., P.B., S.A., N.S., S.T., M.C., A.-M.C., M.-P.C.-C., L.M., and P.G. analyzed data; A.J.S., P.B., S.A., N.S., S.T., M.-P.C.-C., L.M., and P.G. interpreted data; and A.J.S. and P.G. wrote the paper.

The authors declare no conflict of interest.

This article is a PNAS Direct Submission.

[1]Present address: Department of Molecular Biosciences, Northwestern University, Evanston, IL 60208.

[2]To whom correspondence should be addressed. Email: genevaux@ibcg.biotoul.fr.

This article contains supporting information online at www.pnas.org/lookup/suppl/doi:10.1073/pnas.1710456114/-/DCSupplemental.

of 11 single amino acid substitutions in SecB that improve its ability to specifically control *Mtb*-HigBA1 (Fig. 1*B*). Steady-state expression of these mutants was comparable to that of wild-type SecB after 2 h of induction with 50 μM isopropyl β-D-1-thiogalactopyranoside (IPTG) (Fig. S2). To confirm that the improved TA control by the suppressors, herein named SecB^{TA}, was antitoxin-dependent and not related to an indirect effect on the toxin alone, we coexpressed the *Mtb*-HigB1 toxin and the SecB^{TA} variants in the absence of the antitoxin and show that, indeed, none of the SecB variants inactivate *Mtb*-HigB1 toxicity without *Mtb*-HigA1 (Fig. S2).

The localization of the mutations carried by the SecB^{TA} suppressors on the available structure of the *E. coli* SecB tetramer (13) is presented in Fig. 1*C*. The substitutions identified herein are located on strands β1 (T10A, R15H/L), β3 (V64I/L), and β4 (E77V); on the cross-over loop between strands β1 and β2 (Q33L); and in helix α1 (P103L, R111C, I114F, V118L). Residues T10, Q33, V64, and E77 were shown to be involved in substrate binding, and T10 and E77 were shown to additionally contact SecA (14–16). These mutations could directly affect SecB substrate binding specificity, thus increasing functional interaction with *Mtb*-HigA1. Interestingly, mutations at position E77, including the E77V substitution identified here, were previously found to inactivate SecB export function and interaction with SecA (17). However, the well-characterized E77K mutation known to affect SecB export function and interaction with SecA (18) does not improve TA control (Fig. S2). This indicates that export defect through an alteration of SecA binding by SecB is not sufficient to generate TA-specialized SecB and that the E77V substitution may facilitate TA control mainly via modulation of substrate binding.

Among the positions mutated in SecB^{TA} variants that were not previously shown to interact with client proteins, R15, I114, and V118, are in close vicinity to the primary substrate binding site, suggesting that they could also act by modulating the affinity of SecB for *Mtb*-HigA1. The two remaining positions, R111 and P103, are more buried in the structure of the protein, suggesting that mutations of these residues might affect the conformation of SecB to improve antitoxin binding. A detailed structural location of the mutated residues is depicted in Fig. S3. The I114F mutation was largely overrepresented in our genetic selection (i.e., 73 of 116 suppressors carried this substitution), thus suggesting a main role for this position in specialization toward the antitoxin. This residue is located in helix α1 of SecB, in a region that contains a motif highly conserved between SecB family members (Fig. S4), including TACs (3). Positioned directly underneath the main substrate binding surface, I114 was identified by NMR spectroscopy to be in the vicinity of the substrate (either PhoA or MBP), but showed no direct interaction (16). This suggests that residue I114 might be important for the proper structure of the substrate binding site, and mutations at this position could destabilize or somehow remodel the binding site on SecB, thus modulating substrate binding properties (16).

SecB^{I114Y} Is a Bona Fide Specialized SecB^{TA}. Position I114 of SecB likely corresponds to V145 in the sequence of *Mtb*-SecB^{TA} (Fig. S4). However, mutation I114V in the conserved helix α1 motif of

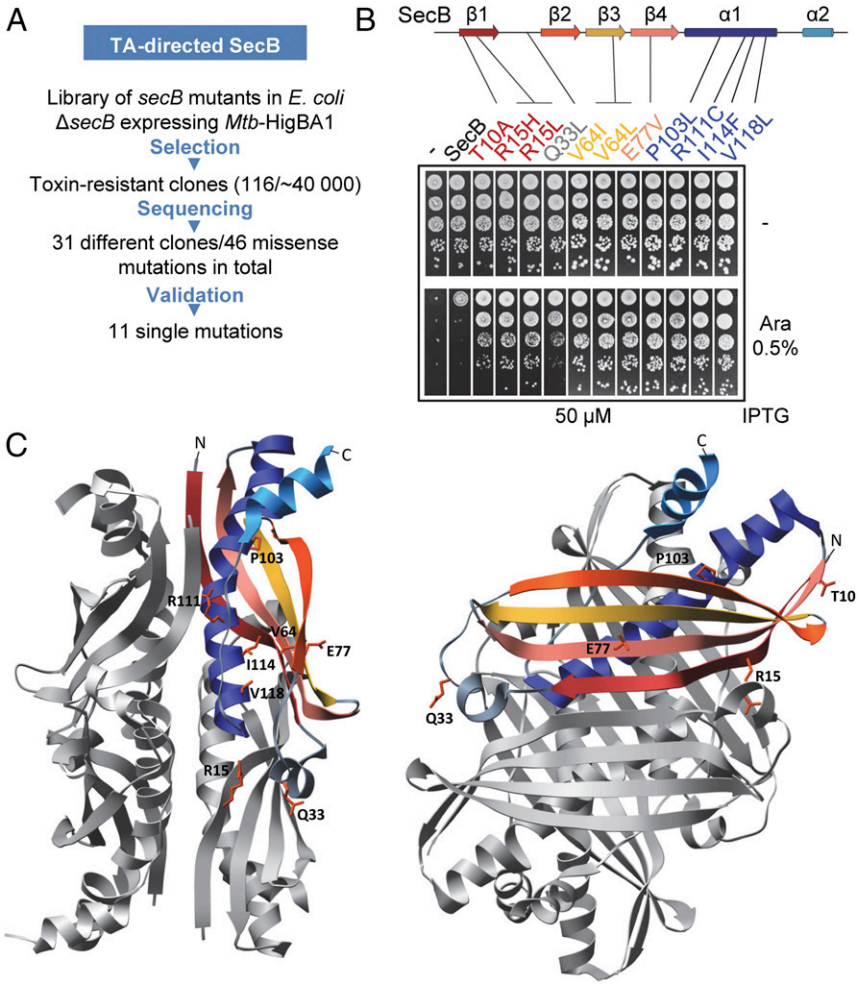

Fig. 1. TA-directed SecB mutants. (*A*) Genetic selection to identify SecB variants with improved ability to control *Mtb*-HigBA1. (*B*) Suppression of *Mtb*-HigBA1 toxicity by SecB^{TA} variants. The position of the suppressors is indicated on SecB secondary structures, with strand β1 in red, strand β2 in orange, strand β3 in yellow, strand β4 in salmon, helix α1 in dark blue, and helix α2 in light blue. W3110 Δ*secB* containing plasmids pK6-*Mtb*-HigBA1 and p29SEN(–), p29-SecB, or p29-SecB^{TA} variant was serially diluted; spotted on agar plates containing arabinose (Ara) and IPTG inducers; and incubated at 37 °C. (*C*) Localization of the mutations isolated on the *E. coli* SecB tetramer (1QYN) in front (*Left*) and side (*Right*) views. Residues are displayed as orange sticks on one SecB monomer, which is colored according to secondary structure elements from *B*.

E. coli SecB does not improve the TA control (Fig. 2*A*). However, residue V145 of *Mtb*-SecB^{TA} is framed by two tyrosines (Fig. S4), and we thus reasoned that introduction of an aromatic residue in this region of SecB could be responsible for the increased TA control function of the SecB^{I114F} variant. Accordingly, mutation I114Y further improves TA control (Fig. 2*A*). Fig. S4 shows the molecular environment of residue I114 in the structures of SecB alone and in complex with PhoA, and illustrates predictions of the structural impact of the mutation to a tyrosine residue at this position. Note that the fact that substitution for a tyrosine was not obtained during the genetic selection procedure is not surprising because I114Y substitution requires two nucleotide changes within the same codon, while all of the mutations isolated resulted from single nucleotide changes. The SecB^{I114Y} mutant, which turned out to be an efficient specialized SecB^{TA} variant, was used to further characterize the mechanism of specialization of SecB toward TA systems.

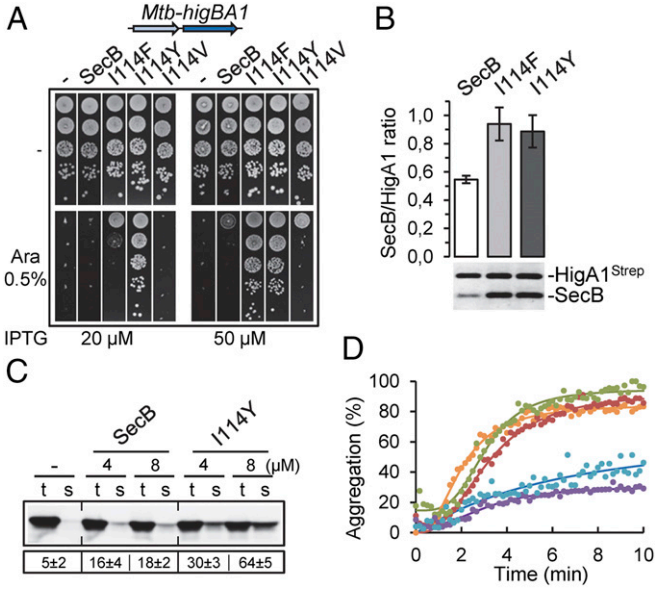

Fig. 2. Specialized SecB^{I114Y} is directed toward *Mtb*-HigA1. (*A*) Suppression of *Mtb*-HigBA1 toxicity. W3110 Δ*secB* containing plasmids pK6-*Mtb*-HigBA1 and p29SEN(–), p29-SecB, p29-SecB(I114F), p29-SecB(I114Y), or p29-SecB(I114V) was serially diluted, spotted on agar plates with or without inducers, and incubated at 37 °C. (*B*) In vivo interaction between *Mtb*-HigA1 and SecB^{TA} variants. W3110 Δ*secB* containing plasmids pK6-*Mtb*-HigA1 and p29-SecB or p29-SecB^{TA} variant was grown to midlog phase, SecB expression was induced with 50 μM IPTG, and *Mtb*-HigA1 was induced with 0.5% arabinose (Ara). Crude cell extracts were mixed with streptactin Sepharose resin, and protein complexes were eluted with desthiobiotin. Protein quantification from elution fractions was carried out after migration on SDS/PAGE, followed by coloration with SYPRO orange using Multi Gauge software. The ratio of SecB/*Mtb*-HigA1 was calculated for each SecB^{TA}. The results are given as fold change normalized to wild-type SecB, and are the mean of three independent experiments. Error bars indicate SD. (*C*) Improved solubilization of newly translated *Mtb*-HigA1 by SecB^{I114Y}. *Mtb*-HigA1 was expressed in a cell-free translation system with or without SecB or SecB^{I114Y} tetramer at 4 μM and 8 μM. After translation, the total (t) and soluble (s) fractions were separated on SDS/PAGE and *Mtb*-HigA1 was revealed by Western blot. The numbers below the electrophoretic pattern represent the mean solubility values (%), calculated by the ratio of the amount of translation products in the s and t fractions obtained from three different translation experiments. The SD is indicated. A representative result of three different experiments is shown. (*D*) Aggregation kinetics of denatured *Mtb*-HigA1 (4 μM) were followed at 30 °C by light scattering at 350 nm without (orange) or with 0.5 μM or 1 μM purified SecB (green and red, respectively) or SecB^{I114Y} (blue and violet, respectively) tetramer.

SecB^{I114Y} Exhibits Enhanced Chaperone Activity Toward *Mtb*-HigA1. We next asked whether evolved SecB had an increased affinity for the antitoxin at steady state, using an in vivo pull-down assay with coexpressed SecB^{TA} variants and strep-tagged *Mtb*-HigA1 antitoxin as bait (9). We found that both SecB^{I114F} and SecB^{I114Y} indeed show an increased interaction with *Mtb*-HigA1, compared with SecB wild type. This is in full agreement with the more robust inhibition of *Mtb*-HigB1 toxicity observed for both TA-directed mutants (Fig. 2*B*). SecB^{I114Y} was then purified and characterized in vitro. Gel filtration analysis confirmed that, as observed for SecB, SecB^{I114Y} forms a tetramer in vitro (Fig. S5). In addition, no difference could be detected between purified SecB and SecB^{I114Y} proteins by circular dichroism or following partial α-chymotrypsin proteolysis (Fig. S5). The ability of purified SecB^{I114Y} and SecB to solubilize *Mtb*-HigA1 in vitro was first investigated using a cell-free coupled transcription/translation assay, as performed previously (11). In this case, a significant fraction of the newly synthesized antitoxin was solubilized by SecB^{I114Y} (up to 64% in the presence of 8 μM chaperone), and to a lesser extent by SecB wild type (up to 18% at the same concentration; Fig. 2*C*). Note that solubilization by SecB^{I114Y} in this assay is not as robust as that observed with the native *Mtb*-SecB^{TA} chaperone, which fully solubilized *Mtb*-HigA1 under the same conditions (11). We next monitored the ability of SecB^{I114Y} and SecB to directly prevent aggregation of denatured *Mtb*-HigA1 in vitro. In this assay, we found that SecB^{I114Y} significantly prevents *Mtb*-HigA1 aggregation, while SecB wild type showed no detectable effect (Fig. 2*D*). In this case, SecB^{I114Y} was nearly as efficient as *Mtb*-SecB^{TA} to prevent the aggregation of *Mtb*-HigA1 (Fig. S6). Together, these results demonstrate that the specialized SecB mutants have been efficiently redirected toward the antitoxin.

Finally, all of the other SecB^{TA} variants identified in this work were also tested for interaction with *Mtb*-HigA1 by pull-down in vivo. As observed for SecB^{I114Y} and SecB^{I114F}, eight of 11 variants show an increased affinity for *Mtb*-HigA1 in vivo (Fig. S7). Variants T10A and R15H were comparable to SecB wild type, and R111C showed reduced binding, somehow suggesting a more transient interaction that may not be detected under the steady-state conditions tested. Accordingly, we purified both SecB^{T10A} and SecB^{R15H} variants and found that they could efficiently prevent *Mtb*-HigA1 aggregation in vitro (Fig. S7), in a manner comparable to that of SecB^{I114Y} (Fig. 2*D*).

Evolved SecB^{TA} Interacts with the Chaperone Addiction Extension of *Mtb*-HigA1. Antitoxins of TAC systems possess a carboxyl-terminal extension named chaperone addiction (ChAD), which is responsible for interaction with the dedicated chaperone and renders TAC antitoxins chaperone-dependent (11). ChAD regions are highly variable in length and amino acid composition, and they present high specificity for their respective SecB^{TA} (11). We took advantage of these findings to investigate whether evolved SecB^{I114Y} mutant is specifically directed toward the ChAD region of *Mtb*-TAC, like *Mtb*-SecB^{TA}. Growth inhibition assays were performed in the presence of SecB^{I114Y} coexpressed with chaperoneless TA pairs of three different TAC systems: *Mmet*-TAC from *Methylomonas methanica*, *Vcho*-TAC from *Vibrio cholerae*, and *Glov*-TAC from *Geobacter lovleyi* (3, 11). Remarkably, SecB^{I114Y} was not capable of assisting the three chaperoneless TA pairs of these systems unless their original ChAD sequences were replaced by the one of *Mtb*-TAC (Fig. 3*A*, compare top and bottom spot tests; control plates of this experiment with no arabinose inducer added are shown in Fig. S8). Furthermore, assistance to chimeric TA pairs by the evolved SecB^{I114Y} mutant is much more robust than that observed with SecB wild type (11). In support of such specific targeting of SecB^{I114Y} to *Mtb*-ChAD, we found that the *Mtb*-HigA1 harboring the double W108A/W137A mutation in ChAD, previously shown to affect interaction with *Mtb*-SecB^{TA}

(11), also inhibits the ability of SecB^{I114Y} to neutralize *Mtb*-HigBA1 (Fig. 3*B*).

We next used differential scanning fluorimetry (DSF) to investigate the thermal stability of SecB and SecB^{I114Y}, and to test whether SecB^{I114Y} and *Mtb*-SecB^{TA} share the same short region of interaction within the ChAD domain of *Mtb*-HigA1 (11). While thermal denaturation of SecB revealed a high melting temperature (T_m) of 71.7 ± 0.1 °C, the SecB^{I114Y} variant exhibited a significantly reduced thermal stability (53.7 ± 0.2 °C; Fig. S8). This suggests that the I114Y mutation might indeed destabilize the substrate binding site of SecB, and thus potentially modulate interaction with the substrate (16). Notably, *Mtb*-SecB^{TA} was also shown to have a significantly lower T_m than *E. coli* SecB (11). We then analyzed the effect of a set of 14 13-mer peptides encompassing the whole *Mtb*-HigA1 ChAD region (Fig. S8) on both SecB wild type and SecB^{I114Y}, as previously described (11). Strikingly, only the C4 and C5 peptides, previously shown to contain the main site of interaction with *Mtb*-SecB^{TA}, were able to induce a significant increase in the T_m of SecB^{I114Y} but not of SecB wild type (Fig. 3*C*). In agreement with the in vivo results presented above, these data further show that SecB^{I114Y} has indeed specialized toward a region within ChAD that is also recognized by the native *Mtb*-SecB^{TA}. In support of such specificity, *Mtb*-HigA1 deleted for amino acids 104–119 comprising peptides C4 and C5 was not rescued by SecB^{I114Y} or SecB (Fig. 3*B*).

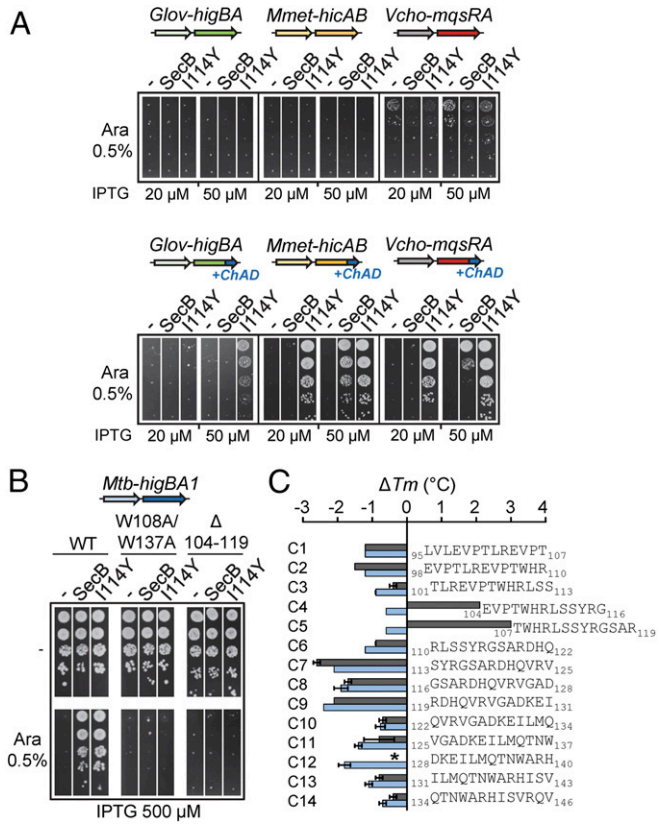

Fig. 3. SecB^{TA} is directed toward the primary ChAD region. (*A*) Functional transfer of the SecB^{I114Y}/*Mtb*-ChAD-specific pair. W3110 Δ*secB* containing the pK6-*Glov*-HigBA, pK6-*Mmet*-HicAB, or pK6-*Vcho*-MqsRA native TA pair (*Top*) or their chimeric derivatives with their respective ChAD sequences being replaced by *Mtb*-ChAD (*Bottom*) was cotransformed with p29SEN-based SecB and SecB^{I114Y} and analyzed by spot tests as in Fig. 1*B*. (*B*) Mutations in ChAD affect suppression by SecB^{I114Y}. W3110 Δ*secB* containing plasmid pK6-*Mtb*-HigBA1, pK6-*Mtb*-HigA1$^{W108A/W137A}$, or pK6-*Mtb*-HigA1$^{Δ(104–119)}$ and p29SEN(–), p29-SecB, or p29-SecB^{I114Y} was spotted on agar plates containing the indicated concentrations of arabinose (Ara) and IPTG inducers, and incubated at 37 °C. (*C*) Thermal stability of SecB and SecB^{I114Y} was monitored by DSF in the presence of each peptide in a 60-fold excess. T_m values were deduced from the fluorescence curves recorded using a temperature gradient from 20 to 90 °C. Shifts in melting temperature are shown for SecB (blue bars) and SecB^{I114Y} (gray bars). Mean and SEM of three replicates are shown. An asterisk (*) indicates no accurate T_m determination. Note that, in most cases, there was no detectable difference between replicates.

Generic Export Functions of Evolved SecB^{TA}. Improving chaperone activity toward a specific substrate generally results in a decreased generic chaperone function (19, 20). We thus asked whether specialized SecB variants fulfill their generic chaperone function at low temperature and in the presence of novobiocin antibiotic, with both reflecting a protein export defect (21, 22). Remarkably, SecB^{I114Y} fully complements for the lack of SecB as efficiently as the wild type (Fig. 4*A* and Fig. S9, respectively). Note that this was also the case for all SecB^{TA} variants isolated, with the exception of the previously described export-deficient variant SecB^{E77V} (Fig. S9). We next followed the maturation kinetics of two SecB substrates by pulse-chase analyses in a *secB* mutant. In this case, expression of SecB^{I114Y} fully restores export of proOmpA and proOmpF to levels comparable to those of wild-type SecB (Fig. 4*B*). Finally, we additionally confirmed that binding of SecB^{I114Y} to SecA was not affected in vitro (Fig. 4*C*). Taken together, these data indicate that evolution toward TA control does not alter the export function of SecB.

Cytosolic Chaperone Functions of SecB^{TA}. SecB overexpression partially suppresses the temperature-sensitive growth and prevents cytosolic protein aggregation in the absence of both cytosolic TF and DnaK chaperones (23). Under these conditions, suppression by SecB is independent of its export function (23). We took advantage of the severe growth phenotype of the *tig dnaKJ* mutant to test our SecB^{TA} variants in vivo and found that none of the SecB mutants identified could suppress the growth defect better than SecB wild type (Fig. S9). On the contrary, seven of 12 SecB^{TA} variants, including SecB^{I114Y}, showed a significantly reduced ability to replace TF and DnaK compared with SecB wild type (Fig. 4*D* and Fig. S9). Accordingly, prevention of cytosolic protein aggregation by SecB^{I114Y} in the absence of TF and DnaK was also less efficient (Fig. 4*E*). These results mirror the previously observed weak suppression of the *tig dnaK* mutant phenotypes by *Mtb*-SecB^{TA} (9). Although the reasons for this are unknown, we cannot exclude the possibility that subtle changes within the substrate binding site of the TA-directed SecB could affect its ability to support bacterial growth in such a stringent context or that the absence of the major DnaK/TF pathway could affect the stability and conformation of certain SecB variants. Notably, all of our previous attempts to improve SecB function in the absence of TF and DnaK using the same SecB mutant library and a selection for growth above 37 °C were unsuccessful. This suggests that improvement of SecB toward cytosolic protein substrates of the TF/DnaK chaperone pathway may not be achievable under the conditions tested. We next asked whether SecB^{I114Y} was also affected in its ability to prevent in vitro aggregation of the model substrate L-malate dehydrogenase (MDH). In this case, SecB^{I114Y} exhibits reduced ability to prevent the aggregation of MDH compared with wild-type SecB (Fig. 4*F*). This is in sharp contrast to the increased aggregation prevention observed for the *Mtb*-HigA1 antitoxin, and indicates that the mutation I114Y has distinct effects on the interaction with different substrates.

Interplay Between Export Function and TA Control. All SecB-like proteins of TAC systems tested so far have retained their ability to efficiently suppress the export defect of an *E. coli secB* mutant, while being specialized toward their cognate ChAD extension (3, 11). This suggests that competitive binding of SecB^{TA} to the antitoxin or to preprotein clients could underlie the mechanism

MICROBIOLOGY

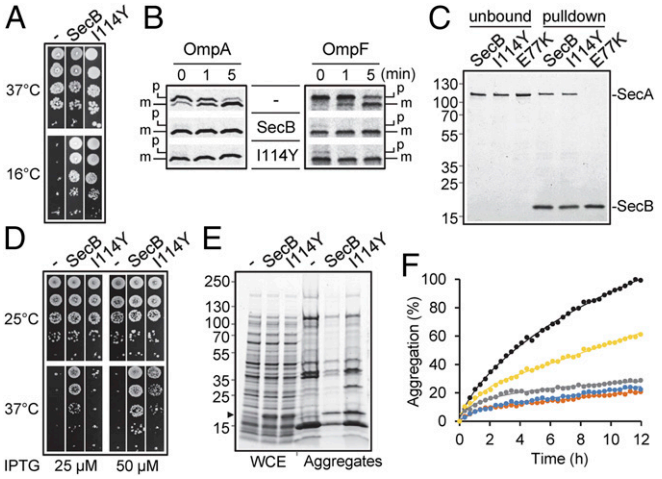

Fig. 4. Generic chaperone functions of TA-directed SecB^{I114Y}. (*A*) W3110 Δ*secB* containing plasmid p29SEN(–), p29-SecB, or p29-SecB(I114Y) was spotted on agar plates at indicated temperatures. (*B*) Pulse-chase analysis showing the processing of radiolabeled proOmpA and proOmpF in the strain W3110 Δ*secB* containing plasmid p29SEN(–), p29-SecB, or p29-SecB(I114Y). Mature (m) and precursor (p) forms of both OmpA and OmpF are shown. (*C*) In vitro interaction of His-tagged SecB, SecB^{E77K} ,and SecB^{I114Y} with Flag-tagged SecA. Pull-down was performed using nickel-nitrilotriacetic acid resin. The unbound and elution (pull-down) fractions are shown. A protein ladder (in kilodaltons) is shown to the left of the gel. (*D*) MC4100 Δ*tig* Δ*dnaKdnaJ* strain containing p29SEN(–), p29-SecB, or p29-SecB(I114Y) was grown to midlog phase at 25 °C; spotted on agar plates containing IPTG inducer as indicated; and incubated at 25 °C or 37 °C. (*E*) Prevention of aggregation in the MC4100 Δ*tig* Δ*dnaKdnaJ* double-mutant strain harboring plasmid pSE380ΔNcoI(–), pSE-SecB, or p2SE-SecB (I114Y). Cells were grown to midlog phase at 25 °C, induced with 0.5 mM IPTG for 1 h, and switched at 33 °C for 1 h, and aggregates were extracted. Whole-cell extracts (WCE) and corresponding aggregate fractions (Aggregates) are shown. The position of SecB is shown with a black arrow. (*F*) In vitro aggregation of L-MDH. Aggregation kinetics of denatured L-MDH (2 μM) were followed at 30 °C by light scattering at 350 nm without (black) or with either 0.25 μM or 0.5 μM SecB (gray and orange, respectively) or SecB^{I114Y} (yellow and blue, respectively) tetramers.

of activation of TAC systems, as proposed (3, 9). We took advantage of the evolved SecB^{I114Y}, which retained its full ability to assist protein export, to test whether the antitoxin and preprotein clients could indeed compete for binding to SecB. We thus asked whether overexpression of the *Mtb*-HigA1 antitoxin could interfere with the export function of TA-specialized SecB mutant. Both SecB and SecB^{I114Y} were coexpressed with the antitoxin in *E. coli* Δ*secB* (9), and export kinetics of proOmpA were measured by pulse-chase analysis (Fig. 5*A*). In the absence of antitoxin, no difference could be detected between SecB and SecB^{I114Y} in the rescuing of OmpA export, confirming that the mutant's export function is kept intact. Strikingly, expression of *Mtb*-HigA1 in these conditions leads to a severe delay of maturation of proOmpA in the case of the TA-directed SecB^{I114Y} mutant, while it has no detectable effect on SecB wild type (Fig. 5*B*). The same result was found with proOmpF substrate (Fig. S10). This indicates that *Mtb*-HigA1 can indeed compete with the export function of specialized SecB^{TA} more than it does with SecB wild type, suggesting that under some circumstances, SecB^{TA} chaperone function might be recruited either by the antitoxin or by accumulation of preproteins.

Discussion

In this work, we have isolated single amino acid substitutions within SecB that significantly improve TA control, thus illustrating the remarkable adaptability of this chaperone. The fact that all SecB-like chaperones of TAC tested so far have kept the ability to perform generic SecB export functions (3, 11) and that a directed evolution toward TA specialization does not impair the export capacity of SecB suggests that SecB^{TA} chaperones might have undergone subfunctionalization, with optimization of a preexisting TA control function and a generic export function unaffected (24). Whether comparable chaperone plasticity can be found in other chaperone families remains unknown. Notably, the HscA member of the Hsp70 chaperone family, which is involved in the biogenesis of iron-sulfur proteins, has specialized toward a conserved "LPPVK" motif within its IscU substrate and, as a consequence, has lost its ability to bind a broad range of substrates and to functionally replace the multifunctional DnaK/Hsp70 homolog (25, 26). Similarly, a directed evolution of GroEL (Hsp60) toward heterologous GFP identified mutations in the chaperone that markedly improved GFP folding but that, in turn, significantly altered its ability to fold natural GroEL substrates and to replace GroEL in vivo (19). Therefore, in contrast to the unaffected SecB export function, specialization toward specific substrates severely impacted the main generic chaperone properties of these chaperones.

Analysis of TA-directed SecB revealed that the isolated mutations either affect residues previously known to directly interact with substrate or more buried residues that had not been characterized yet. Substitutions at these buried positions could alter the structure of the tetramer in a way that specifically enhances the productive interaction with the *Mtb*-HigA1 antitoxin, as our results suggest in the case of SecB^{I114Y}. Notably, destabilized variants of the Spy periplasmic chaperone selected on the basis of their ability to stabilize a poorly folded immunity protein 7 mutant have also been isolated (27). However, in this case, the chaperone activity of Spy variants was also improved for all of the other substrates tested. In sharp contrast, SecB^{I114Y} seems to only assist a certain type of substrate, as we observed reduced chaperone activity toward cytosolic substrates in vivo and in vitro and no chaperone activity toward other antitoxins tested in this work. This shows that discreet changes in SecB can readily remodel the chaperone to specifically accommodate very diverse ChAD amino acid extensions that are present in TAC antitoxins. The fact that SecB can bind long stretches of polypeptides on its remarkably large substrate binding surface (over 7,600 Å^2) indeed suggests that subtle changes within this surface could modulate the interaction with

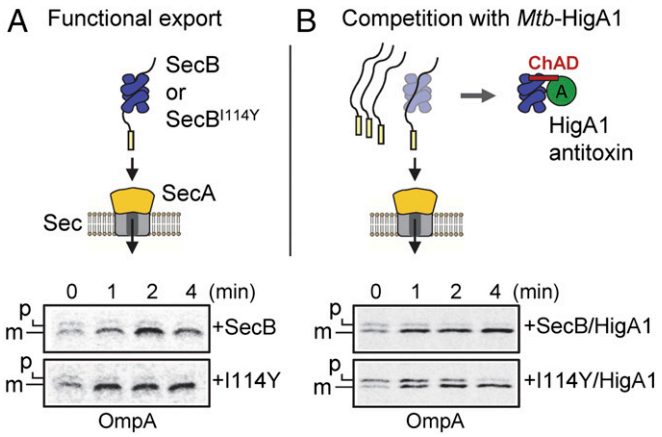

Fig. 5. *Mtb*-HigA1 can compete with the export function of specialized SecB. Pulse-chase analysis showing the processing of the radiolabeled OmpA precursor (p) or mature (m) form in the strain W3110 Δ*secB* expressing SecB or SecB^{I114Y} without (*A*) or with (*B*) coexpressed *Mtb*-HigA1. Cells were grown at 30 °C to midlog phase, and were induced with 50 μM IPTG and with 0.002% arabinose 30 min later. After 30 min, cultures were switched to 18 °C, pulse-labeled, and chased for the indicated times. Samples were immunoprecipitated with anti-OmpA antibodies, separated by SDS/PAGE, and analyzed by autoradiography.

specific substrates without affecting the binding to presecretory proteins (16, 28).

Directed evolution of molecular chaperones has been successfully employed to enhance the folding of aggregation-prone proteins involved in neurodegenerative diseases (29). For example, mutations in the middle domain of the yeast Hsp104 disaggregase improve its ability to rescue proteotoxicity in models of Parkinson's disease and amyotrophic lateral sclerosis (30). The remarkably adjustable substrate selectivity of SecB suggests that this chaperone might be easily genetically manipulated to accommodate new substrates, including aggregation-prone disease proteins or other heterologous proteins for biotechnology purposes.

Materials and Methods

Bacterial Strains and Culture Conditions. Genetic experiments were performed in *E. coli* strains W3110 Δ*secB*::Cm^R (21) and MC4100 Δ*tig*::Cm^R Δ*dnaKdnaJ*::Kan^R (31). Bacteria were grown in LB or M9 medium supplemented with ampicillin (100 or 50 μg/mL when specified), chloramphenicol (15 μg/mL), or kanamycin (40 μg/mL) when necessary.

Genetic Selection. To construct a SecB mutant library, the *secB* gene was amplified by error-prone PCR, cloned as an EcoRI/HindIII fragment into plasmid p29SEN under an IPTG-inducible promoter, and transformed in *E. coli* DH5α. Approximately 15,000 transformants were pooled, and plasmids were extracted. Sequencing of random clones from the library indicates that the rate of mutations in *secB* was two (eight mutations for 467 bp). To select for TA-specific SecB mutants, the W3110 Δ*secB*::Cm^R strain containing pK6-*Mtb*-HigBA1 was transformed with the p29SEN-based library of SecB mutants and grown at 37 °C on LB ampicillin/kanamycin agar plates supplemented with 0.5% arabinose and 50 μM IPTG to induce expression of the TA system and SecB, respectively. Note that under these conditions, transformation with the plasmid p29-SecB expressing SecB wild type did not produce any viable colony on plates. A control aliquot of transformants plated on LB ampicillin/kanamycin agar plates without inducer indicates that the number of transformants tested during the selection was ∼40,000. Plasmids that confer bacterial growth in the presence of inducer were independently extracted from a total of 120 colonies, retransformed in *E. coli* DH5α strain, and selected on LB ampicillin agar plates. Kanamycin-sensitive colonies were selected, grown in LB ampicillin, and subjected to plasmid extraction. Plasmids were retransformed in W3110 Δ*secB*::Cm^R cells containing pK6-*Mtb*-HigBA1 and tested for suppression in the presence of 0.5% arabinose and 50 μM IPTG inducers. The suppressors that passed the second round of selection (n = 116) were sequenced using primers pSE-For (5′-gtgtggaattgtgagcggat-3′) and pSE-Rev (5′-gatttaatctgtatcaggctg-3′).

Bacterial Growth Assays. *E. coli* strain W3110 Δ*secB*::Cm^R was cotransformed with pK6-*Mtb*-HigBA1 and p29SEN, p29-SecB, or p29-SecB^{TA} variant on LB ampicillin/kanamycin agar plates containing 0.2% glucose at 37 °C. Fresh transformants were grown in LB ampicillin/kanamycin to midlog phase, serially diluted, and spotted on LB ampicillin/kanamycin agar plates with or without IPTG and arabinose inducers as indicated. Plates were incubated at 37 °C overnight. For complementation of SecB chaperone activity in vivo, fresh transformants of W3110 Δ*secB*::Cm^R containing p29SEN-based constructs were grown at 37 °C to midlog phase in LB ampicillin, serially diluted, and spotted on LB ampicillin agar plates in the absence or presence of IPTG inducer. Plates were incubated for 1 d at 37 °C or for 5 d at 16 °C. For growth complementation using the MC4100 Δ*tig*::Cm^R Δ*dnaKdnaJ*::Kan^R temperature-sensitive strain (32), midlog-phase cultures of fresh transformants grown at 25 °C in LB ampicillin (50 μg/mL) were serially diluted and spotted on LB ampicillin (50 μg/mL) agar plates at 25 °C and 37 °C with or without IPTG inducer.

Details about plasmid constructs, pull-down assays, pulse-chase analysis, protein purification, DSF, aggregation assays, circular dichroism, chymotrypsin proteolysis, and cell-free protein synthesis are given in *SI Materials and Methods*.

ACKNOWLEDGMENTS. We thank Charalampos Babis Kalodimos (University of Minnesota) for discussion and Gianluca Cioci and Bertrand Delahaye for technical assistance. The DSF equipment and the spectropolarimeter are part of the Integrated Screening Platform of Toulouse (PICT, IBiSA). This work was supported by the Ministère de l'Education Nationale de la Recherche et de la Technologie and the Fondation pour la Recherche Médicale Grants FDT20140930836 (to A.J.S.), UPS-2014-113 (to S.A.), ANR-13-BSV8-0010-01 (to L.M. and P.G.), and SNF CRSII3_160703 (to P.G.).

1. Sala A, Bordes P, Genevaux P (2014) Multitasking SecB chaperones in bacteria. *Front Microbiol* 5:666.
2. Randall LL, Hardy SJ (2002) SecB, one small chaperone in the complex milieu of the cell. *Cell Mol Life Sci* 59:1617–1623.
3. Sala A, Calderon V, Bordes P, Genevaux P (2013) TAC from Mycobacterium tuberculosis: A paradigm for stress-responsive toxin-antitoxin systems controlled by SecB-like chaperones. *Cell Stress Chaperones* 18:129–135.
4. Gerdes K, Christensen SK, Løbner-Olesen A (2005) Prokaryotic toxin-antitoxin stress response loci. *Nat Rev Microbiol* 3:371–382.
5. Lewis K (2010) Persister cells. *Annu Rev Microbiol* 64:357–372.
6. Van Melderen L (2010) Toxin-antitoxin systems: Why so many, what for? *Curr Opin Microbiol* 13:781–785.
7. Helaine S, et al. (2014) Internalization of Salmonella by macrophages induces formation of nonreplicating persisters. *Science* 343:204–208.
8. Soo VW, Wood TK (2013) Antitoxin MqsA represses curli formation through the master biofilm regulator CsgD. *Sci Rep* 3:3186.
9. Bordes P, et al. (2011) SecB-like chaperone controls a toxin-antitoxin stress-responsive system in Mycobacterium tuberculosis. *Proc Natl Acad Sci USA* 108:8438–8443.
10. Sala A, Bordes P, Genevaux P (2014) Multiple toxin-antitoxin systems in Mycobacterium tuberculosis. *Toxins (Basel)* 6:1002–1020.
11. Bordes P, et al. (2016) Chaperone addiction of toxin-antitoxin systems. *Nat Commun* 7:13339.
12. Schuessler DL, et al. (2013) Induced ectopic expression of HigB toxin in Mycobacterium tuberculosis results in growth inhibition, reduced abundance of a subset of mRNAs and cleavage of tmRNA. *Mol Microbiol* 90:195–207.
13. Dekker C, de Kruijff B, Gros P (2003) Crystal structure of SecB from Escherichia coli. *J Struct Biol* 144:313–319.
14. Crane JM, et al. (2005) Mapping of the docking of SecA onto the chaperone SecB by site-directed spin labeling: Insight into the mechanism of ligand transfer during protein export. *J Mol Biol* 353:295–307.
15. Lilly AA, Crane JM, Randall LL (2009) Export chaperone SecB uses one surface of interaction for diverse unfolded polypeptide ligands. *Protein Sci* 18:1860–1868.
16. Huang C, Rossi P, Saio T, Kalodimos CG (2016) Structural basis for the antifolding activity of a molecular chaperone. *Nature* 537:202–206.
17. Kimsey HH, Dagarag MD, Kumamoto CA (1995) Diverse effects of mutation on the activity of the Escherichia coli export chaperone SecB. *J Biol Chem* 270:22831–22835.
18. Fekkes P, et al. (1998) Preprotein transfer to the Escherichia coli translocase requires the co-operative binding of SecB and the signal sequence to SecA. *Mol Microbiol* 29:1179–1190.
19. Wang JD, Herman C, Tipton KA, Gross CA, Weissman JS (2002) Directed evolution of substrate-optimized GroEL/S chaperonins. *Cell* 111:1027–1039.
20. Aponte RA, Zimmermann S, Reinstein J (2010) Directed evolution of the DnaK chaperone: Mutations in the lid domain result in enhanced chaperone activity. *J Mol Biol* 399:154–167.
21. Ullers RS, Ang D, Schwager F, Georgopoulos C, Genevaux P (2007) Trigger factor can antagonize both SecB and DnaK/DnaJ chaperone functions in Escherichia coli. *Proc Natl Acad Sci USA* 104:3101–3106.
22. Nichols RJ, et al. (2011) Phenotypic landscape of a bacterial cell. *Cell* 144:143–156.
23. Ullers RS, et al. (2004) SecB is a bona fide generalized chaperone in Escherichia coli. *Proc Natl Acad Sci USA* 101:7583–7588.
24. Sahi C, et al. (2013) Sequential duplications of an ancient member of the DnaJ-family expanded the functional chaperone network in the eukaryotic cytosol. *Mol Biol Evol* 30:985–998.
25. Hesterkamp T, Bukau B (1998) Role of the DnaK and HscA homologs of Hsp70 chaperones in protein folding in E.coli. *EMBO J* 17:4818–4828.
26. Hoff KG, Ta DT, Tapley TL, Silberg JJ, Vickery LE (2002) Hsc66 substrate specificity is directed toward a discrete region of the iron-sulfur cluster template protein IscU. *J Biol Chem* 277:27353–27359.
27. Quan S, et al. (2014) Super spy variants implicate flexibility in chaperone action. *Elife* 3:e01584.
28. Crane JM, et al. (2006) Sites of interaction of a precursor polypeptide on the export chaperone SecB mapped by site-directed spin labeling. *J Mol Biol* 363:63–74.
29. Jackrel ME, Shorter J (2017) Protein-remodeling factors as potential therapeutics for neurodegenerative disease. *Front Neurosci* 11:99.
30. Jackrel ME, et al. (2014) Potentiated Hsp104 variants antagonize diverse proteotoxic misfolding events. *Cell* 156:170–182.
31. Bruel N, et al. (2012) Hsp33 controls elongation factor-Tu stability and allows Escherichia coli growth in the absence of the major DnaK and trigger factor chaperones. *J Biol Chem* 287:44435–44446.
32. Genevaux P, et al. (2004) In vivo analysis of the overlapping functions of DnaK and trigger factor. *EMBO Rep* 5:195–200.
33. Sakr S, et al. (2010) Lon protease quality control of presecretory proteins in Escherichia coli and its dependence on the SecB and DnaJ (Hsp40) chaperones. *J Biol Chem* 285:23506–23514.
34. Tomoyasu T, Mogk A, Langen H, Goloubinoff P, Bukau B (2001) Genetic dissection of the roles of chaperones and proteases in protein folding and degradation in the Escherichia coli cytosol. *Mol Microbiol* 40:397–413.
35. Bordoli L, et al. (2009) Protein structure homology modeling using SWISS-MODEL workspace. *Nat Protoc* 4:1–13.